ELSEVIER

Journal of Organometallic Chemistry 565 (1998) 243–258

Journal of Organometallic Chemistry

Diferrocenyltriphosphines 1: five-coordinate ruthenium complexes[1]

Ian R. Butler [a,*], Ulrich Griesbach [a], Piero Zanello [b], Marco Fontani [b], David Hibbs [c], Michael B. Hursthouse [c], K.L.M. Abdul Malik [c]

[a] *Department of Chemistry, University of Wales, Bangor, Gwynedd, LL57 2UW, UK*
[b] *Dipartimento di Chimica dell'Universita di Siena, Pian dei Mantellini, 44-53100 Siena, Italy*
[c] *EPSRC Crystallographic Centre, Cathedral Park, PO Box 912, Park Place, Cardiff, CF1 3TB, UK*

Received 1 January 1998

Abstract

The ligand bis-1-(1′-diphenylphosphinoferrocenyl)phenylphosphine, triphosfer, reacts with dichlorotris-triphenylphosphineruthenium(II) to give the complex [(triphosfer)$RuCl_2$], (**17**), in almost quantitative yield. This complex reacts with CO at ambient temperature to afford [(triphosfer)$Ru(CO)Cl_2$]. Three related complexes, [{(η-$R_2PC_5H_4$)Fe–μ^2-(η-$C_5H_4P(R')$η-C_5H_4)Fe(η-$C_5H_4R_2$)}$RuCl_2$], R,R′ = Ph, *i*Pr (**18–20**), exhibit identical chemical properties. Reaction of complexes **17–20** with excess PMe_2Ph results in the deligation of the ferrocene ligand. The electrochemistry shows that while the diferrocenyltriphosphine ligands undergo a single two-electron oxidation, irreversible in character, complexes (**17–19**) exhibit two separated one-electron oxidations having features of chemical reversibility. This data suggests that while within the ligands no electronic communication exists between the two ferrocene subunits, complexation with $RuCl_2$ allows communication between the two ferrocenes. The single crystal X-ray structure of [(triphosfer)$RuCl_2$] has been determined.

Keywords: Synthesis; Ferrocene; Phosphine; Ruthenium(II); Electrochemistry; Crystal structure

1. Introduction

The preparation and use of ferrocene-based ligands has gained considerable momentum in the past 5 years or so following on from the early chemistry which was developed almost a quarter of a century ago. Arguably the most important ligand of all the ferrocene-based compounds is the bdppf(dppf) **1** which was initially prepared by Sollot et al. [1] and was later used by Davison in 1971 [2]. This ligand has been widely used in both coordination studies and as a ligand in transition metal-based catalysts [3,4]. Modification of the ligand by tailoring the phosphorus substituents has been carried out to a significant extent with the preparation of derivatives of the general form **2**. Changing the phosphorus substituents changes both the steric and electronic features of the ligand which in turn is reflected in significant differences in the rates of catalysis of derived complexes (catalyst precursors).

In related chemistry we have previously examined the coordination chemistry of ferrocenylamine ligands of the type **3** with ruthenium [5]. The five-coordinate complexes of the type **4** are obtained directly from the ligands on treatment with [$Ru(PPh_3)_3Cl_2$]. Interestingly these complexes react readily with small molecules either quasi-reversibly (H_2) or irreversibly (CO) to produce the appropriate six-coordinate pseudo-octahedral species **5**. In all of these complexes the ferrocene ligands are bidentate and we were interested if the work could be developed to use tripodal ligands to eliminate the extraneous triphenylphosphine ligand from such complexes.

* Corresponding author.

[1] This paper is dedicated to Professor Michael Bruce, a good friend, on the occasion of his 60th birthday.

0022-328X/98/$19.00
PII S0022-328X(98)00505-1

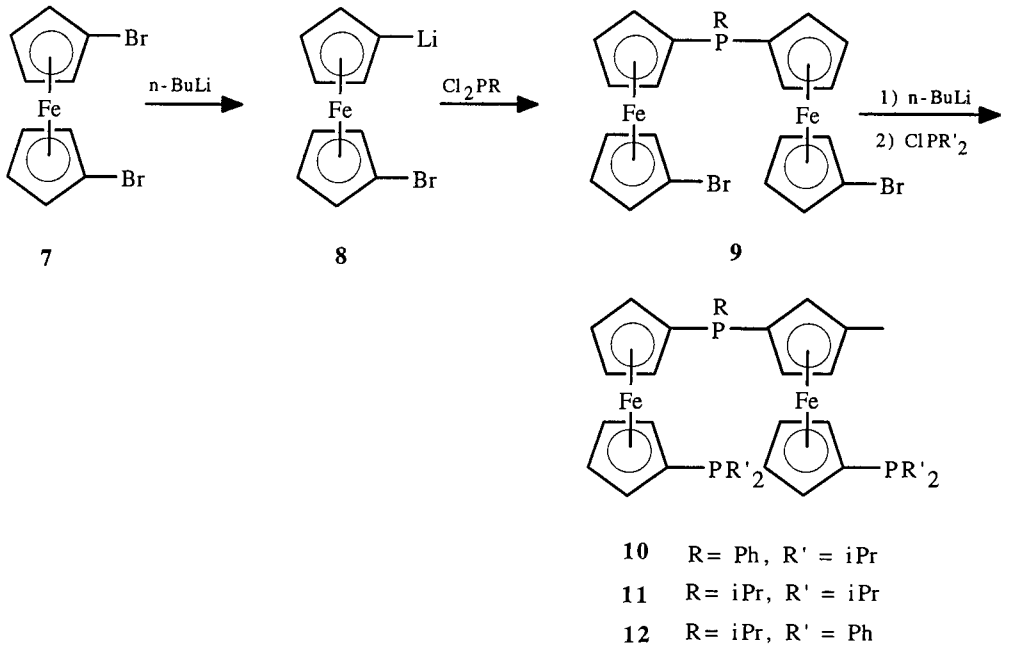

Scheme 1. Tripodal diferrocenyltriphosphine ligand synthetic scheme.

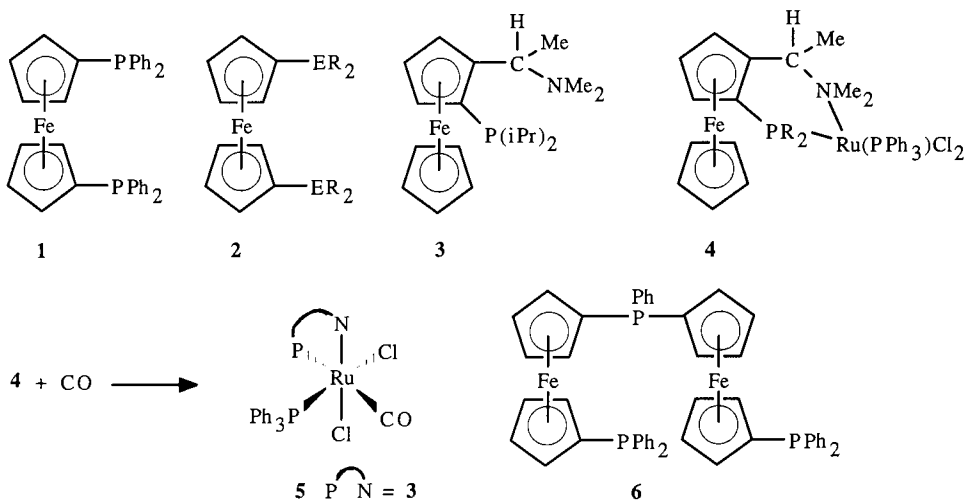

In recent work we have published the synthesis of tripodal diferrocenyltriphosphine ligands, such as triphosfer **6** [6]. The synthetic scheme developed is a relatively simple one beginning with 1,1′-dibromoferrocene as a key precursor (Scheme 1).

We have been able to successfully adapt the methodology to obtain a broad range of ferrocenylphosphine ligands with secondary functional groups. In this work we present the first of these modifications and we present a more rigorous treatment of the ligand characterisation with the preparation of some key ruthenium complexes which derive from the tripodal ligands. Electrochemical and crystallographic structural characterisations have also been carried out.

2. Experimental

2.1. General experimental details

All reactions were carried out under an inert (N_2 or Ar) atmosphere. Chromatography was carried out under aerobic conditions rapidly to avoid oxidation of phosphine ligands. Mass spectra were recorded on either Finnegan 4500 or Finnegan 8200 instruments at the University of Wales, Bangor or University of Wales, Swansea (EPSRC Central Service), and peaks are reported as m/z (relative intensity). ^{1}H-, ^{13}C- and ^{31}P-NMR data were obtained using a Brüker WM250 instrument operating at 250, 62.9 and 101.3 MHz,

Table 1
Crystal data and details of data collection and structure refinement for $[C_{50}H_{41}Cl_2Fe_2P_3Ru]\cdot 2CHCl_3$ (1)

Empirical formula	$[C_{50}H_{41}Cl_2Fe_2P_3Ru]\cdot 2CHCl_3$
Formula weight	1257.14
Temperature (K)	150(2)
Wavelength (Å)	0.71069
Crystal system	Monoclinic
Space group	$P2_1/c$
Unit cell dimensions	
a (Å)	12.555(2)
b (Å)	23.182(4)
c (Å)	17.691(2)
β (°)	105.180(9)
Volume (Å^3)	4969.3(13)
Z	4
$D_{calc.}$ (g cm^{-3})	1.680
Absorption coefficient (mm^{-1})	1.441
$F(000)$	2528
Crystal size (mm)	$0.22\times0.18\times0.14$
Theta range for data collection (°)	1.76–25.04
Index ranges	$-14\le h\le 9$, $-26\le k\le 27$, $-21\le l\le 21$
Reflections collected	20 163
Independent reflections	7505 ($R_{int}=0.0877$)
Absorption correction factors	0.839–0.997
Refinement method	Full-matrix least-squares on F^2
Data/restraints/parameters	7505/0/595
Goodness-of-fit on F^2	0.764
Final R indices [$I>2\sigma(I)$]	[a] $R_1=0.0359$, [b] $wR_2=0.0725$
R indices (all data)	$R_1=0.0632$, $wR_2=0.0759$
Largest difference peak and hole (e Å^{-3})	0.753 and −0.488

[a] $R_1=\Sigma(F_o-F_c)/\Sigma(F_o)$.
[b] $wR_2=[\Sigma\{w(F_o^2-F_c^2)^2\}/\Sigma\{w(F_o^2)^2\}]^{0.5}$; $w=1/[\sigma^2(F_o^2)]$.

respectively[2]. ^{31}P-NMR data is reported relative to 85% H_3PO_4 as internal standard. All solvents were pre-dried and were freshly distilled prior to use. Ferrocene was used as obtained from commercial suppliers, as were the reagents dichlorophenylphosphine and chlorodiphenylphosphine. Other phosphines were prepared according to methods previously used by us following adaption of literature procedures [6]. Chromatography was carried out on silica gel 60–80 mesh unless reported otherwise. TLC data were similarly obtained using silica gel coated glass plates. Materials and apparatus for electrochemistry have been described elsewhere [7]. All potential values are referenced to the saturated calomel electrode (SCE).

[2] In the solvent $CDCl_3$, carbon resonances, in some cases, mask ferrocene carbon resonances. In addition, because of the proximity of the ferrocenyl carbon resonances to each other, it is difficult to distinguish between individual resonances and phosphorus couplings.

Table 2
Atomic coordinates ($\times10^4$) and equivalent isotropic displacement parameters (Å$^2\times10^3$) for $[C_{50}H_{41}Cl_2Fe_2P_3Ru]\cdot 2CHCl_3$ (**1**)

Atom	x	y	z	U_{eq}
Ru(1)	7145.3(6)	1033.1(2)	2673.3(2)	14(1)
Fe(1)	7041.1(6)	−170.4(3)	4538.7(4)	19(1)
Fe(2)	9913.8(6)	1985.6(3)	4136.5(4)	17(1)
Cl(1)	5588.8(10)	1493.7(5)	1814.1(6)	20(1)
Cl(2)	8657.2(10)	375.1(5)	2955.4(6)	22(1)
P(1)	6000.7(11)	214.6(6)	2627.8(7)	17(1)
P(2)	7348.6(10)	1266.8(5)	3912.2(6)	14(1)
P(3)	8242.3(10)	1763.8(5)	2370.7(7)	16(1)
C(1)	6235(4)	−319(2)	3405(3)	22(1)
C(2)	5536(4)	−472(2)	3900(3)	28(1)
C(3)	6093(4)	−900(2)	4439(3)	27(1)
C(4)	7112(4)	−1029(2)	4270(3)	26(1)
C(5)	7208(4)	−673(2)	3637(3)	23(1)
C(6)	7517(4)	673(2)	4613(2)	17(1)
C(7)	6850(4)	556(2)	5146(2)	23(1)
C(8)	7389(5)	112(2)	5673(3)	30(1)
C(9)	8373(4)	−31(2)	5476(3)	27(1)
C(10)	8448(4)	296(2)	4822(3)	22(1)
C(11)	8549(4)	1707(2)	4440(2)	16(1)
C(12)	9536(4)	1513(2)	5002(2)	20(1)
C(13)	10143(4)	1998(2)	5324(3)	22(1)
C(14)	9563(4)	2499(2)	4981(3)	24(1)
C(15)	8589(4)	2317(2)	4445(3)	21(1)
C(16)	9647(4)	1892(2)	2964(2)	16(1)
C(17)	10130(4)	2442(2)	3212(2)	21(1)
C(18)	11154(4)	2359(3)	3747(3)	27(1)
C(19)	11340(4)	1759(2)	3847(3)	23(1)
C(20)	10418(4)	1470(2)	3369(2)	19(1)
C(21)	4527(4)	349(2)	2443(3)	18(1)
C(22)	4149(4)	659(2)	3000(3)	23(1)
C(23)	3051(4)	819(2)	2849(3)	34(1)
C(24)	2329(4)	691(2)	2144(3)	39(2)
C(25)	2684(4)	382(3)	1590(3)	47(2)
C(26)	3794(4)	207(2)	1729(3)	32(1)
C(27)	6066(4)	−224(2)	1776(3)	23(1)
C(28)	5778(5)	−797(2)	1712(3)	36(2)
C(29)	5738(5)	−1093(3)	1019(4)	52(2)
C(30)	5986(5)	−825(3)	407(3)	46(2)
C(31)	6322(5)	−262(3)	472(3)	41(2)
C(32)	6339(4)	41(2)	1155(3)	29(1)
C(33)	6251(4)	1694(2)	4171(2)	14(1)
C(34)	6395(4)	1872(2)	4952(3)	19(1)
C(35)	5599(4)	2169(2)	5187(3)	21(1)
C(36)	4616(4)	2318(2)	4646(3)	25(1)
C(37)	4478(4)	2162(2)	3868(3)	28(1)
C(38)	5294(4)	1853(2)	3634(3)	20(1)
C(39)	8373(4)	1518(2)	1417(2)	17(1)
C(40)	9218(4)	1153(2)	1357(3)	27(1)
C(41)	9250(4)	906(2)	659(3)	35(2)
C(42)	8417(5)	1010(2)	−14(3)	33(1)
C(43)	7551(4)	1369(2)	40(3)	30(1)
C(44)	7517(4)	1620(2)	735(3)	24(1)
C(45)	7747(4)	2501(2)	2207(2)	17(1)
C(46)	8239(4)	2905(2)	1803(2)	21(1)
C(47)	7959(4)	3473(2)	1769(3)	28(1)
C(48)	7183(4)	3665(2)	2130(3)	32(2)
C(49)	6658(4)	3281(2)	2523(3)	34(2)
C(50)	6950(4)	2707(2)	2561(3)	21(1)
C(01)	2986(4)	2103(2)	1623(3)	28(1)
Cl(01)	3751.6(13)	2745.6(7)	1658.4(9)	52(1)
Cl(02)	1905.6(13)	2209.5(7)	2071.3(7)	39(1)

Table 2 (Continued)

Atom	x	y	z	U_{eq}
Cl(03)	2471.0(12)	1873.9(8)	652.4(7)	49(1)
C(02)	9152(4)	−667(3)	1699(3)	41(2)
Cl(04)	10497.8(12)	−380.3(7)	2041.2(9)	52(1)
Cl(05)	8992.0(15)	−935.0(9)	748.2(10)	78(1)
Cl(06)	8903.6(16)	−1196.4(7)	2318.5(12)	70(1)

U_{eq} is defined as one third of the trace of the orthogonalized U_{ij} tensor.

2.2. Preparation of bis-1-(1′-diphenylphosphinoferrocenyl)phenylphosphine (triphosfer), **6**

Bis-1-(1′-bromoferrocenyl)phenylphosphine (3.61 g, 5.68 mmol) was dissolved in anhydrous THF (50 cm^3). The solution was cooled to −70°C (−78° external acetone/dry ice bath) and the mixture was treated with *n*-BuLi (5.0 cm^3 of a 2.5 M solution in hexanes, 12.5 mmol, 2.2 equivalents). After 5 min the reaction was quenched with chlorodiphenylphosphine (2.30 cm^3, 12.5 mmol, 2.2 equivalents). After warming to room temperature (r.t.) the reaction mixture was treated with water (30 cm^3) and diethyl ether (20 cm^3). The organic fraction was separated, dried over anhydrous $MgSO_4$ and reduced to an oil following filtration. The crude concentrate was purified by flash chromatography on silica. Initial elution with petrol (b.p. 40–60°C) removed non-polar by-products. Elution with a mixture of petrol and diethyl ether (1:1, v/v) followed by evaporation of the solvent from the eluted yellow fraction left 3.31 g (60%) of an amber oil which crystallized to leave a voluminous yellow orange solid, m.p. 96–100°C (lit. 124–126°).

$R_f = 0.32$ (petrol:Et_2O = 12:1, v/v). ^{1}H-NMR ($CDCl_3$, 250 MHz): δ 3.86 (m, 2H, ferrocenyl H), (3.99, m, 2H, fc-H), 44.03 (m, 2H, fc-H), 4.07 (m, 2H, fc-H), 4.25 (m, 2H, fc-H), 4.31 (m, 2H, fc-H), 4.34 (m, 2H, fc-H), 4.42 (m, 2H, fc-H), 7.20–7.87 (br, m, 25H, Ph, C_6H_5). {^{1}H}^{31}P-NMR ($CDCl_3$, 100 MHz): δ −32.42 (s, 1P, fc_2P), −17.94 (s, 2P, fcP). {^{1}H}^{13}C-NMR ($CDCl_3$, MHz): δ 71.54, 71.59, 72.25, 72.34, 72.42, 72.51, 72.71, 73.41, 73.63, 73.66, 73.88, 128.05, 128.15, 128.41, 128.48, 133.18, 133.31, 133.48, 133.63, 138.94, 138.79.

The ligands **10, 11** and **12** were prepared using an identical method. The ligands **11** and **12** were isolated initially as oils and in the latter case the oil solidified only on standing for 8 days. Characterisational data is as previously described [6].

Table 3
Selected bond lengths (Å) and angles (°) for $[C_{50}H_{41}Cl_2Fe_2P_3Ru]\cdot 2CHCl_3$ (1)

Bond lengths (Å)			
Ru(1)–P(2)	2.2067(12)	Ru(1)–P(3)	2.3322(14)
Ru(1)–P(1)	2.3688(14)	Ru(1)–Cl(2)	2.3838(13)
Ru(1)–Cl(1)	2.3903(12)	Fe(1)–C(10)	2.019(5)
Fe(1)–C(1)	2.026(4)	Fe(1)–C(5)	2.030(5)
Fe(1)–C(6)	2.040(5)	Fe(1)–C(7)	2.046(5)
Fe(1)–C(8)	2.047(5)	Fe(1)–C(9)	2.049(5)
Fe(1)–C(3)	2.049(5)	Fe(1)–C(2)	2.054(5)
Fe(1)–C(4)	2.055(5)	Fe(2)–C(20)	2.031(5)
Fe(2)–C(17)	2.026(5)	Fe(2)–C(16)	2.024(4)
Fe(2)–C(11)	2.031(5)	Fe(2)–C(15)	2.032(5)
Fe(2)–C(12)	2.036(5)	Fe(2)–C(13)	2.044(4)
Fe(2)–C(14)	2.046(5)	Fe(2)–C(19)	2.055(5)
Fe(2)–C(18)	2.052(5)	P(1)–C(1)	1.814(5)
P(1)–C(21)	1.819(5)	P(1)–C(27)	1.837(5)
P(2)–C(6)	1.827(5)	P(2)–C(33)	1.849(5)
P(2)–C(11)	1.856(5)	P(3)–C(45)	1.816(5)
P(3)–C(16)	1.825(4)	P(3)–C(39)	1.829(5)
C(1)–C(5)	1.439(7)	C(1)–C(2)	1.439(7)
C(2)–C(3)	1.426(7)	C(3)–C(4)	1.420(7)
C(4)–C(5)	1.422(7)	C(6)–C(7)	1.442(6)
C(6)–C(10)	1.429(6)	C(7)–C(8)	1.434(7)
C(8)–C(9)	1.409(7)	C(9)–C(10)	1.405(7)
C(11)–C(15)	1.414(7)	C(11)–C(12)	1.443(6)
C(12)–C(13)	1.392(6)	C(13)–C(14)	1.420(7)
C(14)–C(15)	1.402(6)	C(16)–C(20)	1.431(6)
C(16)–C(17)	1.431(7)	C(17)–C(18)	1.397(6)
C(18)–C(19)	1.415(7)	C(19)–C(20)	1.410(6)
Bond angles (°)			
P(2)–Ru(1)–P(3)	97.35(5)	P(2)–Ru(1)–P(1)	98.15(5)
P(3)–Ru(1)–P(1)	164.47(4)	P(2)–Ru(1)–Cl(2)	94.04(4)
P(3)–Ru(1)–Cl(2)	91.55(5)	P(1)–Ru(1)–Cl(2)	86.41(5)
P(2)–Ru(1)–Cl(1)	112.62(5)	P(3)–Ru(1)–Cl(1)	87.89(4)
P(1)–Ru(1)–Cl(1)	87.05(4)	Cl(2)–Ru(1)–Cl(1)	153.19(4)
C(1)–P(1)–C(21)	102.0(2)	C(1)–P(1)–C(27)	102.2(2)
C(21)–P(1)–C(27)	102.1(2)	C(1)–P(1)–Ru(1)	122.9(2)
C(21)–P(1)–Ru(1)	116.6(2)	C(27)–P(1)–Ru(1)	108.3(2)
C(6)–P(2)–C(33)	101.4(2)	C(6)–P(2)–C(11)	97.9(2)
C(33)–P(2)–C(11)	98.1(2)	C(6)–P(2)–Ru(1)	116.9(2)
C(33)–P(2)–Ru(1)	118.51(14)	C(11)–P(2)–Ru(1)	120.1(2)
C(45)–P(3)–C(16)	100.2(2)	C(45)–P(3)–C(39)	104.9(2)
C(16)–P(3)–C(39)	106.0(2)	C(45)–P(3)–Ru(1)	121.5(2)
C(16)–P(3)–Ru(1)	121.7(2)	C(39)–P(3)–Ru(1)	100.7(2)
C(5)–C(1)–C(2)	107.0(4)	C(5)–C(1)–P(1)	124.2(4)
C(2)–C(1)–P(1)	128.8(4)	C(3)–C(2)–C(1)	107.9(5)
C(4)–C(3)–C(2)	108.5(5)	C(3)–C(4)–C(5)	108.0(5)
C(4)–C(5)–C(1)	108.4(5)	C(7)–C(6)–C(10)	106.9(4)
C(7)–C(6)–P(2)	127.0(4)	C(10)–C(6)–P(2)	125.3(4)
C(8)–C(7)–C(6)	107.7(5)	C(9)–C(8)–C(7)	107.6(5)
C(10)–C(9)–C(8)	109.2(5)	C(9)–C(10)–C(6)	108.5(5)
C(15)–C(11)–C(12)	106.5(4)	C(15)–C(11)–P(2)	125.1(3)
C(12)–C(11)–P(2)	127.9(4)	C(13)–C(12)–C(11)	108.1(4)
C(12)–C(13)–C(14)	108.7(4)	C(15)–C(14)–C(13)	107.5(4)
C(14)–C(15)–C(11)	109.2(4)	C(20)–C(16)–C(17)	106.2(4)
C(20)–C(16)–P(3)	127.0(4)	C(17)–C(16)–P(3)	126.1(4)
C(18)–C(17)–C(16)	109.0(5)	C(17)–C(18)–C(19)	108.2(5)
C(18)–C(19)–C(20)	108.1(4)	C(19)–C(20)–C(16)	108.5(4)

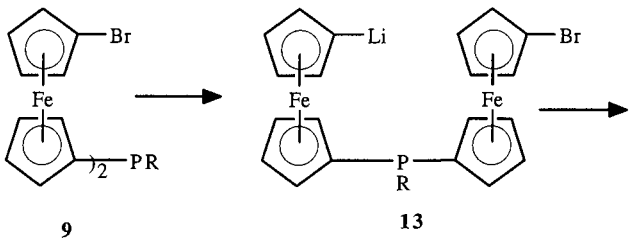

9 13

Scheme 2. Production of compound **13** from compound **9**.

2.3. 1-(1′-Bromoferrocenyl)-1-(1′-diphenylphosphino-ferrocenyl)phenylphosphine, *snowdonphos*, ***14***

Bis-1-(1′-bromoferrocenyl)phenylphosphine (3.00 g, 4.72 mmol) in anhydrous THF (20 cm^3), cooled to ca −70°C was treated with *n*-BuLi (1.90 cm^3 of a 2.5 M solution in hexane, 4.72 mmol, one equivalent). The 4.37 (m, 1H), 4.39 (m, 1H), 7.27–7.42 (brm, 13H, Ph-H), 7.42–7.56 (brm, 2H, PPh-*o*-H). ^{31}P-NMR ($CDCl_3$, 100 MHz): δ −32.60 (s, 1P, fc_2P), −17.83 (s, 1P, fcP). {^{1}H}^{13}C-NMR: 68.36, 68.87, 70.90, 71.54, 73.26, 73.88, 74.52 (overlapping last two resonances) 127.89, 128.27, 128.70, 130.03, 133.18, 133.35, 133.49, 133.60, 133.90 (many overlapped). Anal. Calc. for $C_{38}H_{31}BrFc_2P_2$: C 61.6, H 4.2. Found: C 63.4, H 4.8%. High resolution mass spectrum (FAB) *m*/*z* calc. for $C_{38}H_3P_2Fc_2Br$ 741.976272. Found 741.976405.

2.4. 1-(1′-Diphenylphosphinoferrocenyl)-1-(1′-diisopropylphosphinoferrocenyl)-phenylphosphine, *dppfdipf*, ***15***

To 1-(1′-bromoferrocenyl)-1-(1′-diphenylphosphino-ferrocenyl)phenylphosphine (1.14 g, 1.54 mmol) in anhydrous THF (20 cm^3) maintained at −70°C, was added a *n*-BuLi (0.74 cm^3 of a 2.5 M solution in hexane, 1.84 mmol, 1.20 equivalents). After 10 min the reaction mixture was quenched with chlorodiisopropylphosphine (0.28 g, 1.84 mmol, 1.20 equivalents). Diethyl ether (18 cm^3) was then added to facilitate layer separation, followed by water (10 cm^3). Following the separation of the organic layer and drying over anhydrous $MgSO_4$ the fraction was reduced to a crude oil. The product fraction was eluted using a mixture of petroleum spirit (b.p. 40–60°C) and diethylether(9:2, v/v). Evaporation in vacuo gave the target compound as an orange oil (0.35 g, 29%). Residual 1-(1′-bromoferrocenyl) - 1 - (1′ - diphenylphosphino - ferrocenyl) phenylphosphine (0.57 g, 50%) was also recovered.

R_f 0.50 (petrol:Et_2O, 1:2, v/v). ^{1}H-NMR ($CDCl_3$, 250 MHz): δ 1.10 (2d, 12H, CH_3's), 1.90 (brm, 2H, CH-H), 3.85 (m, 1H, fc-H), 3.92 (m, 2H, fc-H), 4.10 (m, 5H, fc-H), 4.13–4.35 (brm, 8H, fc-H), 7.30 (m, 13H, Ph-H), 7.40–7.60 (brm, 2H, PPh-*o*-H). ^{13}C-NMR: δ 13.63, 19.97, 68.99, 69.83, 70.47, 71.09, 71.56, 71.80, 71.97, 72.69, 72.83, 73.38, 76.51, 77.02, 127.80, 127.92, 128.02, 128.14, 128.40, 128.53, 128.74, 133.16, 133.31, 133.47, 133.62, 134.00, 134.13, 138.53, 138.72, 138.94, 139.10. {^{1}H}^{31}P-NMR: −31.02 (s, Pfc_2Ph), −16.83 (s, PPh_2fc), 0.82 (s, $P(iPr)_2fc$).

2.5. [Ru(***L-15***)Cl_2]

A solution of [$Ru(PPh_3)_3Cl_2$] (958 mg, 1 mmol) and **L-15** (800 mg, 1.03 mmol) in ethanol (10 cm^3) was refluxed for 20 min. On cooling, the solvent was removed under high vacuum and the residue was extracted and filtered with hot hexane. The insoluble brown powder was further washed with hot hexane (2 × 25 cm^3) to give the product complex as a brown/violet powder.

For [Ru(**L-15**)Cl_2]: ^{1}H-NMR ($CDCl_3$): δ 0.6–1.0 (2 dd's, overlapping, 12H), 2.82 (spt, 1H), 3.05 (spt, 1H), 3.38 (m, 1H, fc-H), 3.76 (m, 1H, fc-H), 3.83 (m, 1H, fc-H), 3.86 (m, 1H, fc-H), 3.93 (m, 1H, fc-H), 3.97 (m, 1H, fc-H), 4.06 (m, 1H, fc-H), 4.09 (m, 1H, fc-H), 4.28 (2m, 2H, fc-H), 4.40 (m, 1H, fc-H), 4.49 (m, 1H, fc-H), 4.92 (m, 1H, fc-H), 5.18 (m, 1H, fc-H), 5.25 (m, 1H, fc-H), 6.16 (m, 1H, fc-H), 7.09–8.09 (series of m's, 15H). {^{1}H}^{31}P-NMR ($CDCl_3$): δ 38.49 (td, $fcP(iPr)_2$, J_{P-P} = 12 Hz, 322 Hz), 41.90 (td, $fcPPh_2$, J_{P-P} = 322 Hz, 31 Hz), 86.19 (dd, $fcPfc_2$, J_{P-P} = 12 Hz, 31 Hz).

2.6. [Ru(***L-15***)(CO)Cl_2], *in situ*

A solution of [Ru(**L-15**)Cl_2] in $CDCl_3$ was bubbled with CO for 2 min. The solution changed colour from violet to yellow. The product was subsequently characterized in solution.

For [Ru(**L-15**)(*CO)Cl_2]: ^{1}H-NMR ($CDCl_3$): δ 1.10 (dd, 3H), 1.40 (dd, 3H), 1.60 (dd, 6H), (CH_3's), 2.37 (br spt, 1H), 2.42 (br spt, 1H), 3.63 (m, 1H, fc-H), 3.85 (2m, 2H, fc-H), 3.96 (m, 1H, fc-H), 4.02 (m, 1H, fc-H), 4.06 (m, 1H, fc-H), 4.12 (m, 1H, fc-H), 4.27 (m, 1H, fc-H), 4.34 (2m, 2H, fc-H), 4.43 (m, 1H, fc-H), 4.62 (m, 1H, fc-H), 4.89 (m, 1H, fc-H), 5.19 (m, 1H, fc-H), 5.36 (m, 1H, fc-H), 5.44 (m, 1H, fc-H), 6.94 (m, 4H), 7.10–8.00 (m's, 9H), 8.50 (pseudo t, 2H). {^{1}H}^{31}P-NMR ($CDCl_3$): δ −11.24 (pseudo t, Pfc_2), 19.75 (td, PPh_2, J_{P-P} = 33 Hz, 324 Hz), 24.87 (td, $P(iPr)_2$, J_{P-P} = 25 Hz, 324 Hz). IR: ν_{CO} = 1974 cm^{-1}).

2.7. 1-(1′-Diphenylphosphinoferrocenyl)-1-(1′-carboxalatoferro-cenyl)phenylphosphine, *erasmusphos*, ***16***

To 1-(1′-bromoferrocenyl)-1-(1′-diphenylphosphino-

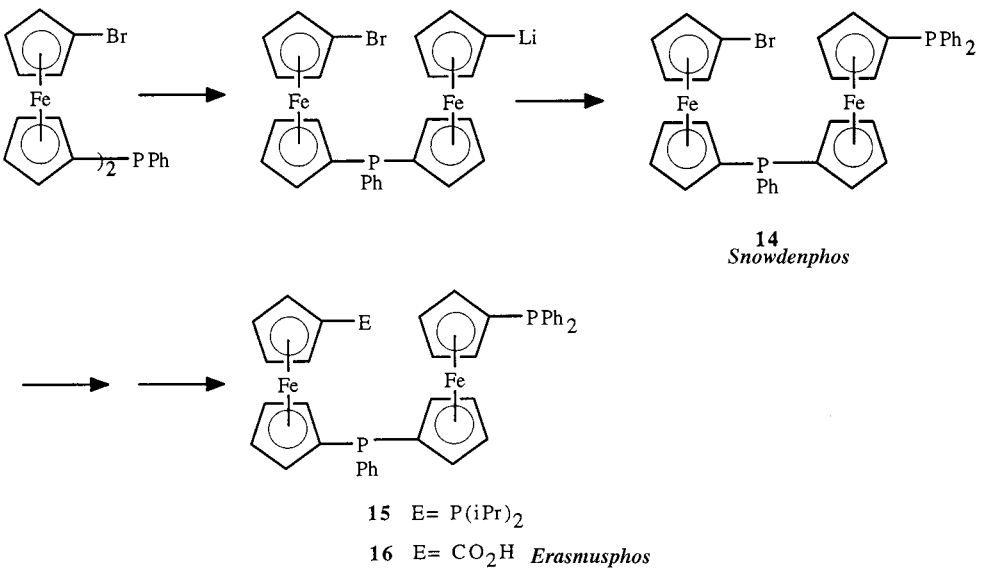

Scheme 3. Production of compounds **14** [1,-(1′-bromoferrocenyl)-1-(1′-diphenylphosphinoferrocene)phenyl phosphine, Snowdonphos], **15** [1-(1′-diphenylphosphinoferrocenyl)-1-(1′-diisopropylphosphinoferrocenyl)-phenylphosphine, dppfdipf] and **16** [1-(1′-diphenylphosphinoferrocenyl)-1-(1′-carboxalatoferrocenyl)phenylphosphine, Erasmusphos] via the intermediate compound **9**.

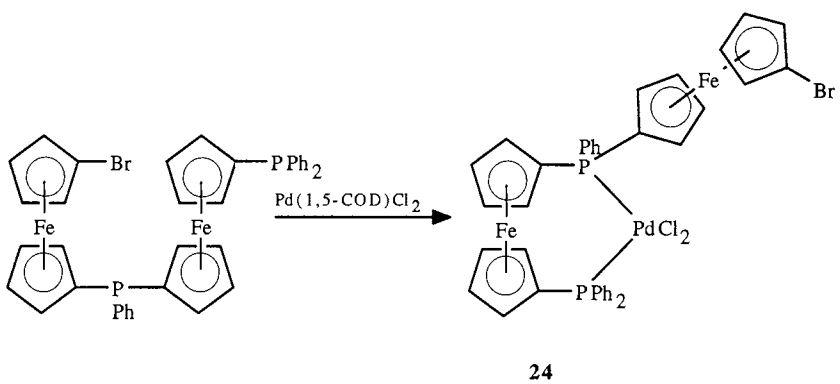

Scheme 4. Production of the palladium complex **24** using [Pd(1,5-COD)Cl_2].

ferrocenyl)phenylphosphine (0.62 g, 0.84 mmol) dissolved in anhydrous THF (8 cm^3) and cooled to ca. −70°C was added *n*-BuLi (0.42 cm^3 of a 2.5 M solution in hexane, 1.09 mmol, 1.30 equivalents). After stirring for 15 min at this temperature, a slow stream of CO_2 was passed through the reaction mixture for 5 min which resulted in the formation of a yellow precipitate from the dark solution. The mixture was allowed to warm to r.t. and was subsequently quenched with a 10% HCl solution (5 cm^3). Diethyl ether was added and the layers were separated. The organic layer was washed with water (2 × 5 cm^3) and brine (5 cm^3). The aqueous layer was extracted with diethyl ether and the combined organic fractions were dried over $MgSO_4$ before being reduced to an oil under vacuum.

The product was isolated from this concentrate following flash chromatography on silica using a mixture of petroleum spirit (b.p. 40–60°C) and diethyl ether (1:1, v/v). Evaporation in vacuo gave (0.10 g, 17%) of an amber oil which solidified on standing.

R_f 0.77 (petrol:Et_2O, 1:1, v/v). ^{1}H-NMR ($CDCl_3$, 250 MHz): δ 3.80 (m, 1H, fc-H), 3.87 (m, 1H, fc-H), 4.00 (m, 1H, fc-H), 4.04 (m, 1H, fc-H), 4.06 (m, 1H, fc-H), 4.09 (m, 1H, fc-H), 4.11-4.15 (m, 2H, fc-H), 4.20 (m, 2H, fc-H), 4.24–4.29 (m, 2H, fc-H), 4.29–4.34 (m, 2H, fc-H), 4.68 (m, 1H, fc-H), 4.76 (m, 1H, fc-H), 7.28 (br m, 13H, Ph-H), 7.45 (br m, 2H, PPh-*o*-H). ^{13}C-NMR: δ 69.03, 70.26, 71.28, 71.29, 71.77, 72.40, 73.08, 73.13, 73.25, 73.37, 73.45, 73.56, 73.67, 73.87, 73.97, 74.01, 74.19, 127.95, 128.06, 128.16, 128.42, 128.50, 129.09. {^{1}H}^{31}P-NMR ($CDCl_3$, 100 MHz): δ −31.91 (s, PPh_2fc), −16.91 (s, Pfc_2Ph).

Table 4
^{31}P chemical shift data on ligation

	Ligand	Unbound	$[RuLCl_2]$	Coordination shift	$[RuL(CO)Cl_2]$	$\triangle^{\neq}$
Pa	Triphosfer, fc_2PPh	−32.10	91.74	+123.84	−8.78	−99.78 *
Pb	Triphosfer, $fcPPh_2$	−17.63	38.33	+55.96	+22.22	−16.11 ○
Pa	**L-10**, fc_2PPh	−31.59	82.40	+113.99	−20.59	−102.99 *
Pb	**L-10**, $fcP(iPr)_2$	+0.08	37.75	+37.67	+21.13	−16.62 ■
Pa	**L-11**, fc_2PiPr	−18.54	77.90	+96.44	+2.77	−75.13 △
Pb	**L-11**, $fcP(iPr)_2$	−0.07	34.06	+34.13	+22.16	−11.90 ■
Pa	**L-12**, fc_2PiPr	−19.03	95.21	+114.24	+8.40	−86.81 △
Pb	**L-12**, $fcPPh_2$	−17.59	34.31	+51.90	+18.05	−16.26 ○
Pa	**L-15**, fc_2PPh	−31.05	+86.19	+117.24	−11.24	−97.43 *
Pb	**L-15**, $fcPPh_2$	−16.83	+41.90	+58.75	+24.87	−17.12 ○
Pb	**L-15**, $fcP(iPr)_2$	+0.82	+38.49	+37.67	+19.75	−18.74 ■

*2.8. Preparation of palladium complex of ligand **14**, **24***

To a solution of $[Pd(COD)Cl_2]$ (200 mg, 0.75 mmol) in the minimum quantity of dichloromethane and ethanol (1:1 v/v) required for dissolution 1:1 equivalent of the ligand **14** was added. The deep red solution obtained was stirred for 1 h before hexane was added which resulted in the precipitation of the product as a deep violet powder which was isolated by filtration and washed with diethyl ether, m.p. > 200°C (decomp). ^{1}H-NMR ($CDCl_3$, 250 MHz): δ 3.65 (m, 1H, fc-H), 3.90 (m, 1H, fc-H), 4.12 (m, 1H, fc-H), 4.29 (brm, 3H, fc-H), 4.48 (br m, 3H, fc-H), 4.50 (br m, 5H, fc-H), 4.72 (m, 1H, fc-H), 4.90 (m, 1H, fc-H), 7.40 (m, 4H, Ph-H), 7.48–7.70 (br m, 6H, Ph-H), 7.82 (m, 1H, Ph-H), 8.05 (m, 1H, Ph-H), 8.25 (m, 3H, Ph-H). MS clusters at m/z 883 $(L\mathrm{PdCl})^+$. $\{^1H\}^{31}$P-NMR: 30.41 (bs), 38.26 (bm).

*2.9. Ruthenium(II). Ru(triphosfer)Cl_2, **17***

Tris-(triphenylphosphine)dichlororuthenium(II) (270 mg, 0.59 mmol) was dissolved in a mixture of ethanol and dichloromethane (40 cm^3, 8:1, v/v) and refluxed for 5 min under N_2. Bis-1-(1′-diphenylphosphinoferrocenyl)phenylphosphine dissolved in a mixture of ethanol and dichloromethane (20 cm^3, 1:1, v/v) was added and the mixture was refluxed for a further 2 h upon which the brown colour changed to black and then red, forming ultimately a brown/red precipitate. Following cooling and solvent reduction to a few cm^3, the precipitate was collected by filtration, was washed with dry diethyl ether and finally dried under vacuum to give 153 mg (25%) of red microcrystals. A low yield caused by subsequent finding that ruthenium sample contained excess triphenylphosphine, after preparation using literature methods [8]. Subsequent preparations using highly purified reagent ruthenium–phosphine complex gave yields in excess of 95%.

M.p. > 240°C (decomp). ^{1}H-NMR ($CDCl_3$, 250 MHz): δ 3.88 (m, 2H, fc-H), 3.99 (m, 2H, fc-H), 4.03 (m, 2H, fc-H), 4.09 (m, 2H, fc-H), 4.28 (m, 2H, fc-H), 4.49 (m, 2H, fc-H), 5.22 (m, 2H, fc-H), 5.95 (m, 2H, fc-H), 7.10–7.40 (br, m, 14H, Ph-H), 7.40–7.52 (br, m, 5H, Ph-H), 7.52–7.62 (br, m, 4H, Ph-H), 7.75 (dd, $J = 10.7$, 7.1 Hz, 2H, PPh-*o*-H). $\{^1H\}^{31}$P-NMR ($CDCl_2$, 100 MHz): δ +38.33 (d, $J = 36$ Hz, 2P, fcP), 91.74 (t, $J = 36$ Hz, 1P, fc_2P). $\{^1H\}^{13}$C-NMR: 68.11, 68.65, 69.34, 74.02, 74.17, 74.32, 78.17 (other resonances masked by solvent), 126.11, 126.28, 126.75, 127.80, 128.35, 129.20, 131.88, 133.94, 135.30, 136.80, 137.01. MS (FAB): clusters at $m/z = 948$ ([Ru(triphosfer)]), 984 ([Ru(triphosfer)Cl]).

An identical methodology was used in the preparation of the complexes [Ru(**L-10**)Cl_2], [Ru (**L-11**)Cl_2] and [Ru(**L-12**)Cl_2].

*2.10. [Ru(**L-10**)Cl_2], **18***

M.p. 295–296°C. ^{1}H-NMR ($CDCl_3$, 250 MHz): δ 1.13 (pq(dd), 6H), 1.30 (pq(dd), 6H), 1.49 (2dd, 12H), 2.98 (m, 4h), 3.38 (m, 4H), 3.73 (m, 2H), 3.92 (m, 2H), 4.03 (t, 2H), 4.16 (t, 2H), 4.34 (m, 2H), 4.48 (t, 2H), 5.10 (t, 2H), 5.45 (t, 2H), 7.13 (td, 2H), 7.26 (m, 2H), 7.92 (dd, 1H). $\{^1H\}^{13}$C-NMR ($CDCl_3$, 75 MHz): δ 190.22, 19.57, 21.57, 22.63, 30.1; 67.20, 68.34, 69.21, 72.06, 72.98, 75.22, 75.34, 125.36, 125.55, 129.62, 136.88, 137.06. $\{^1H\}^{31}$P-NMR ($CDCl_3$, 101 MHz): δ 37.75 (bd), $fcPiPr_2$, 82.40 (bt), fc_2PPh. MS (FAB) calc. for $C_{38}H_{50}Cl_2{}^{56}Fe^{102}RuP_3$ 883.024474. Found 883.020008 ($\Delta = 5.1$ ppm). Anal. Calc. for $C_{38}H_{50}Cl_2Fe_2P_3Ru$: C 52.20, H 4.75. Found: C 52.43, H 5.55%.

*2.11. [Ru(**L-11**)Cl_2], **19***

M.p. 282–283°C. ^{1}H-NMR ($CDCl_3$, 250 MHz): δ 1.06 (pq(dd), 6H), 1.20 (two overlapping dd sets, 12H), 1.48 (m, 12H), 2.60 (spt, 1H), 3.10 (m, 4H), 3.18 (m, 4H), 4.20 (2m, 4H), 4.36 (m, 2H), 4.41 (m, 2H), 4.50 (m, 2H), 4.71 (m, 2H), 5.22 (m, 2H). $\{^1H\}^{13}$C-NMR ($CDCl_3$, 75 MHz): δ 19.98, 19.29, 20.28, 21.67, 21.96,

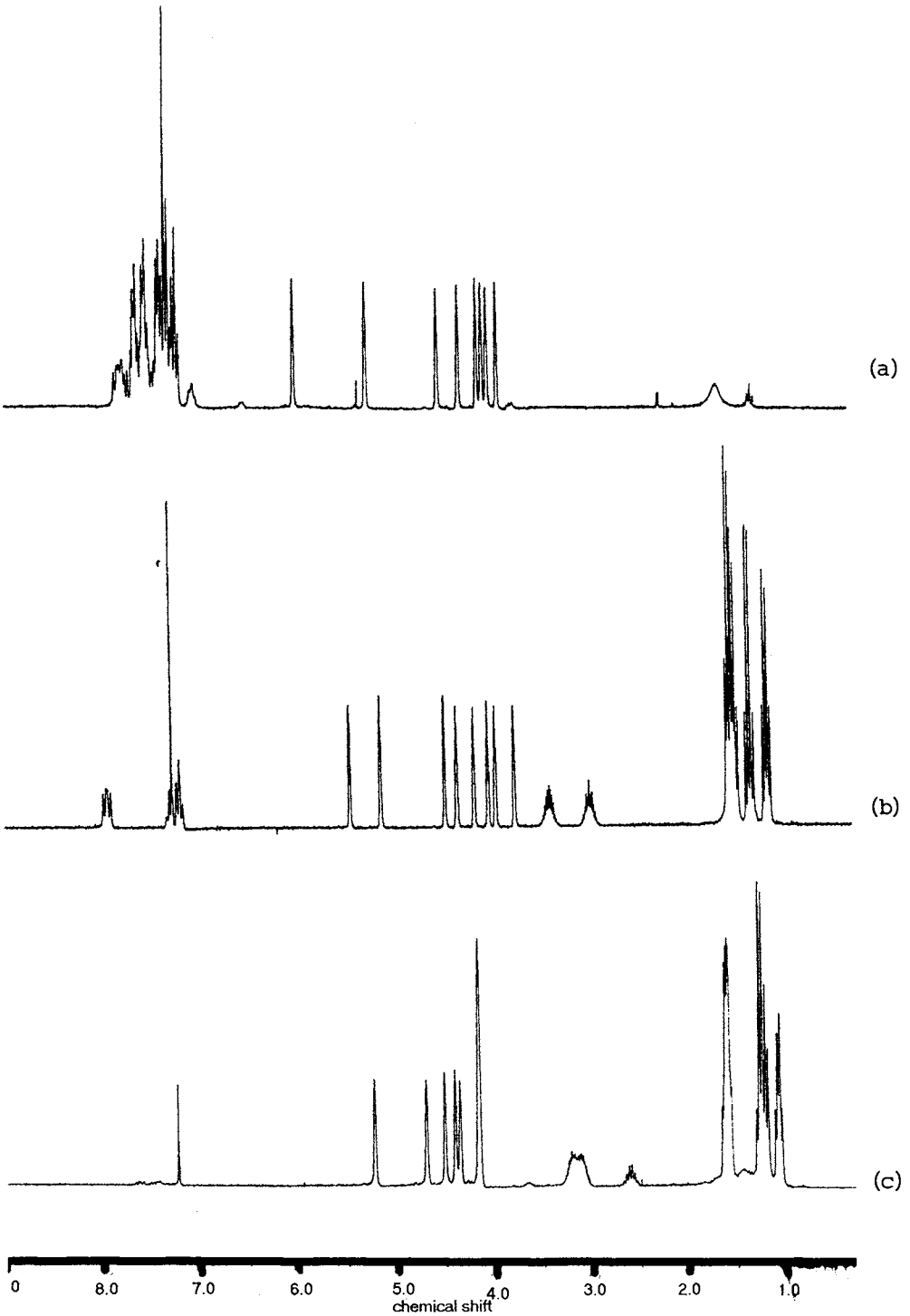

Fig. 1. Comparison of the ^{1}H-NMR spectra of (a) [Ru(**L-6**)Cl_2], (b) [Ru(**L-10**)Cl_2] and (c) [Ru(**L-11**)Cl_2].

23.88, 24.05, 24.21, 29.79, 29.94, 30.09, 31.96, 32.54, 68.61, 68.80, 69.73, 71.92, 72.17, 77.70, 79.70. {^{1}H}^{31}P-NMR ($CDCl_3$, 101 MHz): δ 34.06 (bm)*i*Pr_2*P*fc, 77.90 (bm) fc_2*Pi*Pr. MS calc. for $C_{35}H_{51}Cl_2Fe_2P_3Ru$ 848.03233. Found 848.072306 (Δ = 10 ppm). Anal. Calc. for $C_{35}H_{51}Cl_2Fe_2P_3Ru$: C 49.55, H 6.06. Found: C 49.06, H 5.85%.

*2.12. [Ru(**L-12**)Cl_2], **20***

M.p. 302–303°C (with decomp). ^{1}H-NMR ($CDCl_3$, 250 MHz): δ 1.32 (dd, 6H, $PCHCH_3$), 2.71 (pspt, 1H, PCH), 3.85 (m, 2H, fc-H), 4.06 (m, 2H, fc-H), 4.13 (m, 2H, fc-H), 4.20 (m, 2H, fc-H), 4.44 (m, 2H, fc-H), 4.56 (m, 2H, fc-H), 4.66 (m, 2H, fc-H), 5.81 (m, 2H, fc-H),

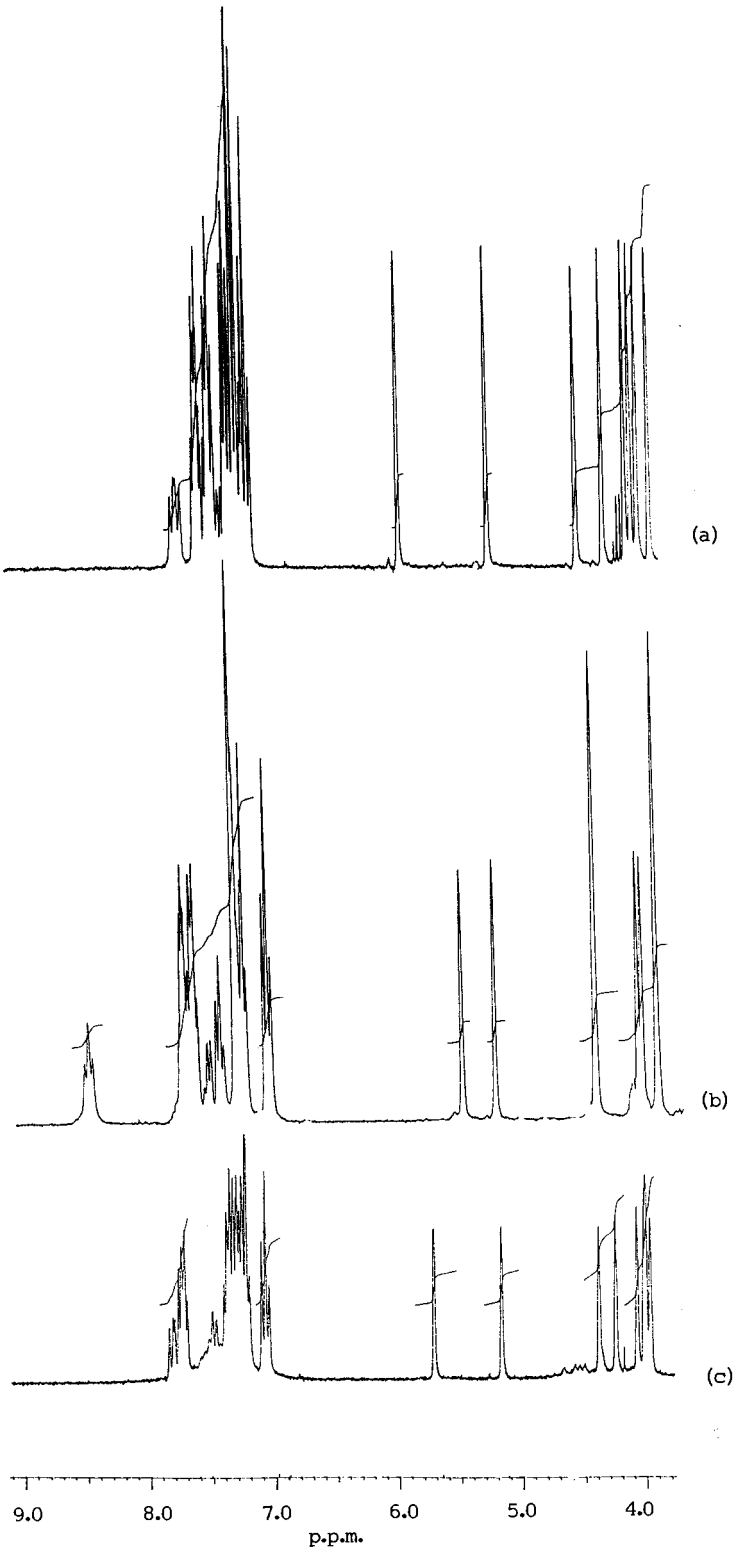

Fig. 2. The change in the proton NMR spectra of (a) [Ru(**L-6**)Cl_2] on transformation to (b) [Ru(**L-6**)(CO)Cl_2]. The spectrum of (c) [Rh(**L-6**)Cl] is shown for comparison.

7.10 (m's, 6H), 7.33 (m's, 6H), 7.56 (m, 4H), 7.80 (m, 4H). $\{^1H\}^{31}P$-NMR: δ 34.31 (d, PPh_2fc), 95.21 (bt, Pfc_2iPr, $J_{P-P} = 29.1$ Hz). Anal. Calc. for $C_{47}H_{43}Cl_2Fe_2P_3Ru$: C 57.34, H 4.40. Found: C 57.54, H 4.25%.

*2.13. Reactions of complexes **17–20** with CO*

The ruthenium complexes in $CDCl_3$ were bubbled with dry CO for 4 min in standard 5 mm NMR tubes. The colour of the solutions, in each case changed to

yellow whereupon the product solutions were characterised by NMR and infrared spectroscopy. In the case of complex **20**, the poorly soluble precursor dissolved readily on CO addition to form the carbonylated product.

2.14. [Ru(triphosfer)(CO)Cl_2], **21**

^{1}H-NMR ($CDCl_3$, 250 MHz): δ 3.91 (m, 4H), 4.07 (m, 2H), 4.12 (m, 2H), 4.45 (m, 4H), 5.24 (m, 2H), 5.52 (m, 2H), 7.11 (pspt, 4H), 7.21–7.88 (m's, 19H), 8.57 (pspt, 2H). {^{1}H}^{13}C-NMR ($CDCl_3$, 75 MHz): δ 68.55, 70.61, 72.12, 72.48, 74.37, 75.60, 77.06, 77.67, 78.17, 78.58, 78.76, 126.84, 127.04, 127.36, 128.15, 128.41, 128.60, 129.40, 124.55, 130.62, 132.01, 132.17, 133.25, 135.65, 138.15, 138.32 (NB; no ^{13}CO observed). {^{1}H}^{31}P-NMR ($CDCl_3$, 101 MHz): δ −8.78 (t, fc_2PPh) J_{P-P} = 30.5 Hz, 22.22 (d, $fcPPh_2$). IR: ν_{CO} = 1988 cm^{-1}.

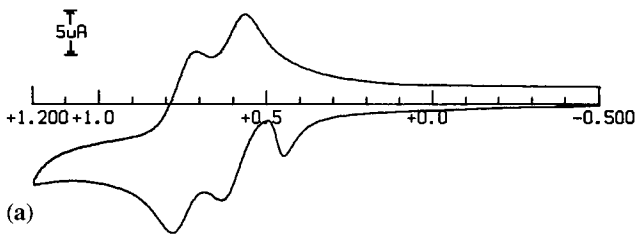

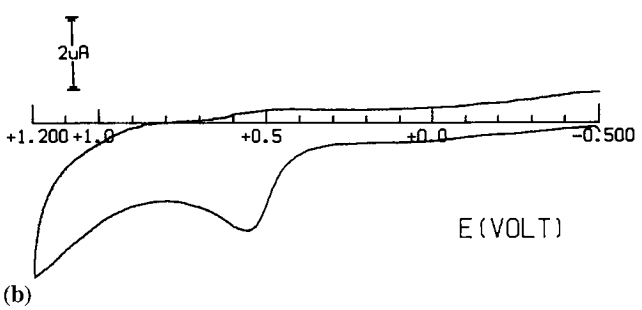

Fig. 3. Cyclic voltammetric responses recorded at a platinum electrode in CH_2Cl_2 solutions containing (a) $[(C_5H_5)Fe(C_5H_4)]_2PPh$ (7×10^{-4} M) and $[NBu_4][ClO_4]$ (0.2 M), and (b) **6** (3×10^{-4} M) and $[NBu_4][PF_6]$ (0.2 M). Scan rate 0.2 V s^{-1}.

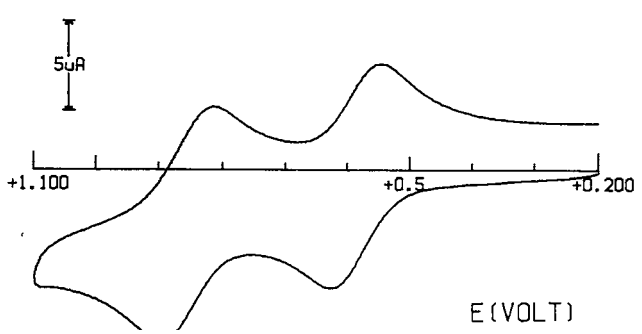

Fig. 4. Cyclic voltammetric response recorded at a platinum electrode in a CH_2Cl_2 solution containing [Ru(**L-6**)Cl_2] (5×10^{-4} M) and $[NBu_3][PF_6]$ (0.2 M). Scan rate 0.2 V s^{-1}.

Table 5
Formal electrode potentials (in V, vs. SCE) and peak-to-peak separation (in mV) for the redox processes exhibited by complexes **17–19** and related molecules in dichloromethane solution with ($[NBu_4][PF_6]$ (0.2 M) supporting electrolyte)

Complex/Ligand	$E^{o\prime}_{0/+}$	ΔE^a_p	$E^{o\prime}_{+/2+}$	Δe^a_p	$E^b_p Ru^{II/0}$
fc_2PPh	+0.60[b]	72	+0.75[b]	76	—
6	+0.56[c]	—	+0.56[c]	—	—
10	+0.49[c]	—	+0.48[c]		—
17	+0.59	69	+0.86	74	−1.6
18	+0.40	76	+0.91	74	−1.6
19	+0.30	74	+0.86	76	−1.6
$Fe(C_5H_5)_2$	+0.39	80	—	—	—

[a] Measured at 0.2 V s^{-1}. [b] $[NBu_4][ClO_4]$ (0.2 M) supporting electrolyte, see text. [c] Peak potential value for irreversible processes.

Table 6
Separations between the two redox potentials (in V) of the bis-ferrocene derivatives reported in Table 5 and Robin–Day classification of their mixed-valent monocations

Complex	$\Delta E^{o\prime}$	K_{com}	Class
$[(C_5H_5)Fe(C_5H_4)]_2PPh$	0.15	3.4×10^2	II
17	0.27	3.7×10^4	II
18	0.51	4.3×10^8	III
19	0.56	3.0×10^9	III

2.15. [Ru(**L-10**)(CO)Cl_2], **22**

^{1}H-NMR ($CDCl_3$, 250 MHz): δ 1.46 (2 dd's, overlapping resonances, 12H), 1.65 (2 dd's, overlapping, 12h), 2.64 (m, 4H, 3.03 (psp, 4H), 3.82 (m, 2H), 4.13 (m, 2H), 4.19 (m, 2H), 4.29 (2m, 4H), 4.50 (m, 2H), 4.97 (m, 2H), 5.22 (m, 2H), 7.35–7.50 (m's, 3H), 8.17 (pst, 2H). {^{1}H}^{13}C-NMR ($CDCl_3$, 75 MHz): δ 18.68, 19.54, 20.35, 20.59, 27.77, 29.38, 68.42, 69.70, 71.90, 73.60, 73.87, 75.96, 126.31, 126.45, 130.03, 138.20, 138.36 (no ^{13}CO observed). {^{1}H}^{31}P-NMR ($CDCl_3$, 101 MHz): δ −20.59 (t) fc_2PPh, 21.13 (d), $fcP(iPr)_2$. IR: ν_{CO} = 1962.2 cm^{-1}.

2.16. [Ru(**L-11**)(CO)Cl_2], **22**

^{1}H-NMR: δ 1.08 (pq(dd), 6H), 1.43 (m's, 15H), 1.82 (pq(dd), 6H), 2.75 (m, 4H), 3.05 (2m's, 5H), 4.20 (2m, 4H), 4.23 (m, 2H), 4.36 (m, 2H), 4.45 (m, 2H), 4.46 (m, 2H), 4.90 (m, 2H), 5.31 (m, 2H). {^{1}H}^{13}C-NMR ($CDCl_3$, 75 MHz): 18.96, 20.37, 20.63, 21.60, 21.63, 23.24 (t), 28.10 (several lines), 68.77, 70.00, 71.39, 72.44, 72.50 (d), 74.21, 74.22 (several overlapping) (N.B. no ^{13}CO observed). {^{1}H}^{31}P-NMR ($CDCl_3$, 101 MHz): δ 2.77 (t) fc_2PiPr, 22.16 $fcP(iPr)_2$. IR: ν_{CO} = 1954.3 cm^{-1}.

2.17. [Ru(**L-12**)(CO)Cl_2], **23**

^{1}H-NMR ($CDCl_3$): δ 1.34 (dd, 6H, $CHCH_3$), 3.25

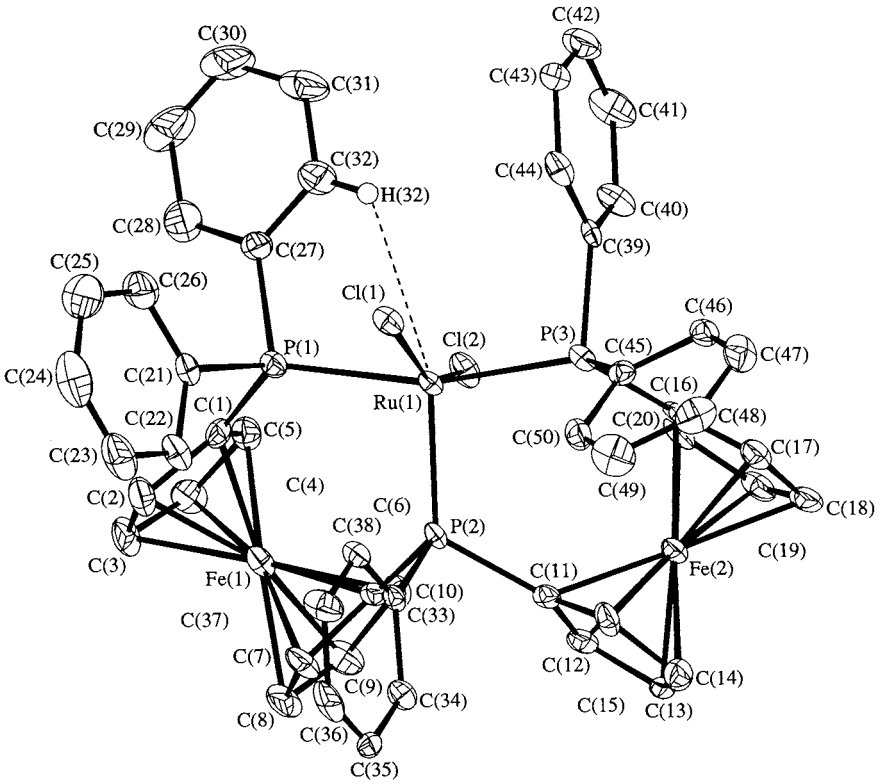

Fig. 5. Structure of [$RuCl_2$(triphosfer)] showing the atom labelling scheme. Thermal ellipsoids are drawn at 50% probability. All hydrogen atoms, except H(32) which blocks the vacant 'octahedral' coordination site around ruthenium, are omitted for clarity.

(bm, 1H), 4.00 (m, 2H, fc-H), 4.15 (m, 2H, fc-H), 4.17 (m, 2H, fc-H), 4.41 (m, 2H, fc-H), 4.51 (m, 2H, fc-H), 4.67 (m, 2H, fc-H), 5.68 (m, 2H, fc-H), 7.18 (m, 4H), 7.37 (overlapping m's, 8H), 7.62 (bm, 4H), 8.05 (bm, 4H). ^{13}C-NMR: δ 20.32, 27.89 (d), 69.01, 70.20, 70.69, 72.00, 73.01, 75.09, 76.52, 78.48, 126.82, 126.44, 127.99, 127.13, 124.83, 130.08, 133.27, 133.34, 133.40, 136.75, 136.88, 136.95 (no ^{13}CO observed). {^{1}H}^{31}P-NMR: δ 8.40 (t, P*i*Prfc), 18.05 (d, PPh_2fc, $J_{P-P} = 30.5$ Hz). IR: $\nu_{CO} = 1974$ cm^{-1}.

2.18. X-ray crystallography

The crystal used for X-ray work was obtained as described above. All measurements were made on a Delft Instruments FAST area detector diffractometer positioned at the window of a rotating anode generator with Mo–K_α radiation ($\lambda = 0.71069$ Å) by following procedures described earlier [9]. The crystal data, details of data collection and structure refinement are summarised in Table 1. The cell parameters were determined by least-squares refinement of diffractometer angles for 250 reflections. The data were corrected for Lorentz and polarisation factors and also for absorption effects (DIFABS) [10].

The structure was solved by direct methods (SHELXS86) [11] and refined by full-matrix least-squares on F^2 using all unique data with intensities greater than zero (SHELXL93) [12]. The non-H atoms were all anisotropic. The H atoms were included in calculated positions (riding model) with $U_{iso} = 1.2 \times U_{eq}$ of the parent carbon. The diagram was drawn using SNOOPI [13]. Sources of scattering factor data are given in ref. [12]. The calculations were done on a 200 MHz personal computer.

Fractional coordinates of the non-H atoms, and selected bond lengths and angles are given in Tables 2 and 3, respectively. Anisotropic displacement coefficients, H atom parameters and complete lists of bond lengths and angles have been deposited as supplementary material.

3. Results and discussion

In the ligand synthetic scheme presented in Scheme 1, it is clear to see that the intermediate compound **9**, by analogy with 1,1′-dibromoferrocene should be amenable to monolithiation in addition to the dilithiation already described in Scheme 2.

The first reaction of this type was carried out at low temperature in THF to avoid Wurtz coupling. The key compound, 1,-(1′-bromoferrocenyl)-1-(1′-diphenylphosphinoferrocene)phenyl phosphine, snowdonphos[3] **14** (Scheme 3), was isolated initially as a yellow/orange oil

[3] The ligand was named due to the similarity of the ^{1}H-NMR spectrum of its palladium complex to the profile of a nearby topological feature.

following column chromatography. The oil originally obtained solidified on standing. The spectroscopic features are unremarkable e.g. ^{31}P δ −32.60, −17.83 which is consistent with diferrocenylphenylphosphines (normally observed at chemical shifts between −24 and −34 δ) and diphenylferrocenylphosphines (−16 to −19 δ). The ^1H-NMR spectrum recorded at 250 MHz is difficult to interpret because of overlap of resonances particularly in the ferrocenyl region, because there are 16 distinct ferrocenyl protons in the racemate. This compound forms the expected palladium complex **24** on treatment with [Pd(COD)Cl_2] (Scheme 4).

Lithiation of snowdonphos followed by a carbon dioxide quench resulted in the formation of the related carboxylic acid derivative **16**, erasmusphos which is obtained as a pale yellow powder following the synthetic procedure and standard work up. Finally a mixed triphosphine ligand was prepared using a chlorodiisopropylphosphine quench sequence to give **15**.

3.1. Tripodal phosphine ligands

As previously mentioned we have described the synthesis of the ligands **6, 10, 11, 12** in a recent paper but we have not discussed the detailed spectral conclusions. To augment the series we have already described the synthesis of **15** in this paper and we have also obtained derivatives of the type **25** by the quench with chlorophenylisopropylphosphine [6].

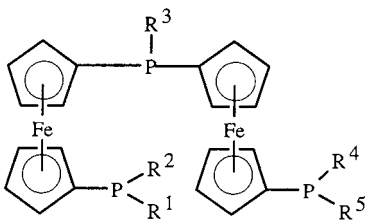

In compound: **6** R_1,R_2,R_3,R_4,R_5 = Ph: **10** R_1,R_2,R_4,R_5 = *i*Pr, R_3 = Ph: **11** R_1,R_2,R_3,R_4,R_5 = *i*Pr: **12** $R_1R_2R_4R_5$ = Ph, R_3 = *i*Pr: **15** R_1,R_2,R_3 = Ph, R_4,R_5 = *i*Pr and **25** R_1,R_3,R_4 = Ph, R_2,R_5 = *i*Pr (racemate).

As a measure of ligand basicity we are able to use the {^1H}^{31}P spectra to give some relative information. There are three distinct variables dependent on the the phosphine substituents which can be classified in tabular form.

The ^{31}P-NMR chemical shift data for five complexes is presented in Table 4. There is an internal consistency in the data allowing for the prediction of chemical shifts with a few ppm according to the nature of the phosphorus substituted. On coordination to ruthenium in the five-coordinated complexes the typical shift for bridgehead (Pa) and terminal (Pb) phosphorus is shown in column 4. The shifts on coordination of CO shown in column 6 show that for similar groups the shift data is also predictable within a few ppm, in most cases.

In the case of triphosfer, on coordination to the '$RuCl_2$' fragment the ligand phosphorus resonances are shifted downfield by ca. 124 and 56 ppm respectively which in comparison with similar coordination with Rh(I) are large [6]. The larger of the shifts is for the unique phosphorus atom, which is as anticipated and the observed J_{P-P} coupling constant is 30 Hz, typical of coupling constants in similar complexes. The larger *trans* coupling, observed in the unsymmetric ligand complex [Ru(**L-15**)Cl_2] is ca. 322 Hz. Typical ^1H-NMR spectra for the complexes [Ru(triphosfer)Cl_2], [Ru(**L-10**)Cl_2] and [Ru(**L-11**)Cl_2] are shown in Fig. 1, illustrating the range of chemical shifts observed in the ferrocenyl region of the spectrum which are dependent on the geometry and donor ability of the phosphorus. By examination of the X-ray structure (following) it is easy to observe the vacant coordination site. On treatment with CO over short periods this free site is rapidly occupied. When this occurs there is again a large shift for the unique phosphorus atom resonance (*trans* to CO, ca. 100 ppm for L = triphosfer), this time upfield, reflecting the increase of electron density on the phosphorus atom. There is also a more reserved effect on the other phosphorus atoms with a modest upfield shift of ca. 16 ppm. The J_{P-P} value is essentially unaffected as the mutual P–P coordination geometry is essentially maintained. The colour of the complex changes from deep red/violet to yellow on CO ligation reflecting the increased crystal field stabilization in the new pseudo octahedral geometry. The ^1H-NMR spectrum before and following CO binding for L = triphosfer are shown in Fig. 2. There are clearly significant chemical shifts of the ferrocenyl resonance on coordination of the ligand reflecting the proximity of the ferrocenyl protons to the metal centre. The carbonyl stretching frequency for the complexes [Ru(**L-6**)(CO)Cl_2], [Ru(**L-10**)(CO)Cl_2], [Ru(**L-11**)(CO)Cl_2], [Ru(**L-12**)(CO)Cl_2] and [Ru(**L-15**)(CO)Cl_2] are observed at 1988, 1962, 1954, 1974 and 1974 cm^{-1}, respectively. Clearly the stretching frequency may be used as a rough guide to ligand basicity with the stronger metal carbonyl interaction observed in the more highly alkyl-substituted phosphines.

A large volume of work has been compiled on the reaction chemistry of complexes of the type [Ru(P_3)Cl_2], P_3 = tripodal phosphine e.g. [CH{$(CH_2)_2PPh_2$}$_3$], **A,** or [PhP{$(CH_2)_2PPh_2$}$_2$], **B** [14]. For example, the complexes of the general type [HRu(P_3)H_2]$^+$ P_3 = **A** are more stable than their diphosphine analogues, and there are many examples of other metal hydride complexes of other transition elements. A series of papers has documented the reaction chemistry of rhenium and rhodium trisphosphine complexes using the unique geometry of the tripodal ligands [15]. The complexes [LRu(P_3)Cl_2], P_3 = **B**, on treatment with hydrides readily afford the dihy-

dride complexes which on protonation form molecular hydrogen complexes [16]. The six-coordinate complexes themselves are obtained on direct treatment of the parent five-coordinate species with appropriate ligands e.g. L = CO, PMe_2Ph, CH_3CN, DMSO, etc.

It is of immediate and relevant interest to find out if a similar reaction chemistry can be developed for the ferrocene-based ligand series. The advantage that such ligands have is that a more rigid ligand backbone should result in highly stabilized complexes with the added ability for such ligands to move electron density from one phosphorus atom to another through the ferrocene backbone to give secondary stabilization. The simple synthesis we have developed for these ligands allows for ease of substitution of the phosphorus with different alkyl or aryl groups allowing facile steric and electronic tuning of the ligand template. Interestingly, treatment of each of the complexes **17–20** with an excess of dimethylphenylphosphine in hot ethanol resulted in complete deligation with the formation of the appropriate ruthenium monodentate phosphine complex. Clearly further chemical studies are warranted in this area. Initial results on the reactions of complexes **17–20** with hydride are inconclusive and are ongoing. The reaction chemistry with pyridinyl bases will be the subject of the next paper in this series.

3.2. Electrochemistry

In order to account for the electrochemical behaviour of the present ruthenium(II) complexes **17–19**, it is useful to illustrate preliminarily the electrochemical responses given by their diferrocenyl ligands themselves. In this connection Fig. 3 compares the cyclic voltametric behaviour of unsubstituted bis-(ferrocenyl)phenyl-phosphine with that of its diphenylphosphino-substituted triphosfer **6** in dichloromethane solution.

As shown, bis-(ferrocenyl)phenylphosphine undergoes two separated oxidations with features of chemical reversibility, which are preceded by a minor adsorption wave. It must be taken into account that such response has been obtained on using $[NBu_4][ClO_4]$ as the supporting electrolyte. As a matter of fact, the use of $[NBu_4][PF_6]$ affords a response displaying a higher prewave ($E_p = +$ 00.43 V) followed by a broad reversible peak-system. These data could account for some uncertainties which still exist about the electrochemical behaviour of bis-(ferrocenyl)phenylphosphine: a simple sequential oxidation of the two ferrocenyl subunits in $CH_2Cl_2/[NBu_4][ClO_4]$ [17] versus a sequential oxidation of the two ferrocenes preceded by a PPh centred anodic process in DMSO/$[NBu_4][BF_4]$ solution [18]. Accordingly, we attribute the prewave to adsorption phenomena more or less pronounced depending upon the solution composition. By contrast, free triphosfer, independent from the nature of supporting electrolyte, undergoes an irreversible oxidation process, which in controlled potential coulometry ($E_w = +0.7$ V) consumes two electrons per molecule. Only at the scan rate of 10 V s^{-1} does the appearance of a directly associated reduction peak take place. We assign such a two-electron step to the concomitant oxidation of the two ferrocene units. Identical behaviour is displayed by ligand **10**. The fact that the addition of the phosphino substituents in the bis-(ferrocenyl)phenylphosphine backbone causes instability of their ferricinium congeners is not unexpected in that for instance 1-diphenylphosphinoferrocene undergoes a chemically reversible one-electron oxidation whereas the oxidation of 1,1′-bis-diphenylphosphinoferrocene is more complex being coupled to chemical complications [19]. The effect of the two PPh_2 substituents is more complex if one considers that a single two-electron step precludes no electronic interaction between the two ferrocene subunits in sharp contrast with what occurs for bis-(ferrocenyl)phenylphosphine.

Fig. 4, which illustrates the anodic portion of the electrochemical response of the ruthenium(II) complex of triphosfer, exemplifies the redox aptitude of the present ruthenium complexes.

As seen, complexation with $RuCl_2$ seems to restore either the electronic communication between the two ferrocene subunits or the stability of the oxidation congeners, in that two separated one-electron oxidations (coulometrically measured) appear again, both having features of chemical reversibility. Nevertheless, the occurrence of the sequential ruthenium centre oxidation Ru(II)/Ru(III)/Ru(IV) cannot be, in principle, ruled out, even if it were accompanied by the disappearance of ferrocene oxidations. In all ruthenium complexes **17–19**, step by step controlled potential electrolysis show that only the corresponding monocations are fairly stable, whereas the dications tend to decompose. An irreversible two-electron reduction is present at very negative potential value, which we confidently assign to the Ru(II)/Ru(0) step.

Table 5 compiles the redox potentials of the present complexes together with those of related derivatives.

The differences between the formal electrode potentials of the subsequent oxidation processes in the present bis-ferrocene molecules are reported in Table 6. Such differences, allowing computation of the relevant comproportionation constants, allow the electrogenerable mixed-valent monocations to be classified according to the Robin–Day classification [20].

As can be seen in Table 6, increasing the electron-donating ability of the peripheral biferrocene–phosphine substituents makes the electronic communication between the two ferrocenes increase progressively from the slightly charge-delocalized class II to the completely charge-delocalized class III.

There are interesting implications of these observations in that it should be possible to adapt the ligands

into conducting polymeric assemblies which could, in theory, be used to sense metal ions because an electronic communication between the iron centres will be established only when the metal ion binds into the coordination pocket.

3.3. X-ray structure of Ru(triphosfer)Cl_2, **17**

The molecular structure of **17** is shown in Fig. 5, which also indicates the crystallographic atom numbering scheme used. Selected molecular geometry parameters are presented in Table 2.

Although there are several reports on the structures of metal complexes containing tridentate PPP donor ligands, the present compound appears to be unique in that it is the first example of a metal compound bound to a tridentate PPP ligand containing two ferrocenyl units (triphosfer). The ruthenium atom is five-coordinate and has a distorted square pyramidal geometry with the bridging phosphorus [P(2)] at the apical position. The main deviations from ideal geometry are the angles (a) P(2)–Ru(1)–Cl(1) which, instead of being ca. 90°, has a value of 112.62(5)°, and (b) P(1)–Ru(1)–P(3) and Cl(1)–Ru(1)–Cl(2) which, instead of 180°, are 164.47(4) and 153.19(4)°, respectively. The much wider P(2)–Ru(1)–Cl(1) angle may be explained by the short Cl(1)···H(38) 2.547 Å steric interaction. The P–Ru–P chelate angles 97.35(5) and 98.15(5)° are comparable with that [99.82(8)°] in the palladium complex [$PdBr(C_{14}H_8Cl)\{Fe(C_5H_4–PPh_2)_2\}$] [21] and are dictated by the 'bite' associated with the ferrocenyl bisphosphine moiety. Other Cl–Ru–P angles lie in the range 86.41(5)–94.04(4)° and closer to 90°.

Besides the present compound, there are only two other five-coordinate ruthenium structures reported to date, which contain the '$RuCl_2PPP$' moiety, i.e. [$RuCl_2$(TTP)] [TTP = $Ph_2P(CH_2)_3P(Ph)(CH_2)_3PPh_2$] [22], and [$RuCl_2$(CyTTP)]·$2Me_2SO$ [CyTTP = $(cyclohexyl)_2P(CH_2)_3P(Ph)(CH_2)_3P(cyclohexyl)_2$] [23]. In the TTP complex, the coordination geometry was described as square pyramidal, whereas a trigonal bipyramidal arrangement was reported for the CyTTP complex, with considerable distortions being observed in both cases. In our compound the two chloride ligands are mutually *trans*, in contrast with their *cis* arrangement in the above two compounds. It may be pointed out that 'RuCl(PPP)' complexes generally prefer six-coordinate octahedral geometry, which may be achieved by the five-coordinate monomeric species taking a 'sixth' ligand or forming a trichloro-bridged dimer in a 'face sharing bioctahedral' arrangement. The first category of these complexes includes [$RuCl_2$ $(ETP)_2$]·$CHCl_3$·Et_2O [ETP = $Ph_2P(CH_2)_2P(Ph)(CH_2)_2PPh_2$] [24], [$RuCl_2$ (ETP)(Me_2SO)]·C_6H_5Me [25], [$RuCl_2$(MTP){P $(OMe)_3$}] [MTP = $Me_2P(CH_2)_3P(Me)(CH_2)_3PMe_2$] [26], [$RuCl_2$(STP)($PMe_3$)] [STP = $(Me_2PCH_2)_3Si(Me)$] [26], and [$RuCl_2$(CMTP)(PPh_3)] [CMTP = $PhP(C_8H_{11})P(Ph)(C_8H_{11})PPh$] [27], whilst the second group includes the $[Ru_2Cl_3(ETP)]^+$ cation in the Ph_4B^- [28] and $F_3CSO_3^-$ [22] salts, and the $[Ru_2Cl_3[TRIPHOS)_2]^+$ cation [TRIPHOS = $(Ph_2PCH_2O)_3C(Me)$] in the Ph_4B^- salt [29]. Of all these complexes, the ETP compound [24] is quite unusual since it contains a monodentate ETP bonded to ruthenium in addition to the usual tridentate ligand. Simpler phosphine ligands are monodentate (PR_3, R = Me, Et, Ph, etc.) or bidentate ($R_2PCH_2PR_2$, R = Me, Et, Ph, etc.) and tend to yield both monomeric and dimeric species depending on the relative size, shape and orientation of the ligands around the metal. An important point to note here is that the five-coordinate ruthenium complexes are extremely useful, since the associated 'coordinative unsaturation' plays a vital role in catalytic property of such materials [30]. In fact two very important catalysts used in homogeneous hydrogenation i.e. $RhCl(PPh_3)_3$ [31] and $RuCl_2(PPh_3)_3$ [32–34] are both 'coordinatively unsaturated' 16-electron species.

The Ru–P distances are different, those to the terminal phosphorus atoms [Ru(1)–P(1) 2.3688(14), Ru(1)–P(3) 2.3322(14) Å] being significantly longer that to the central atom [Ru(1)–P(2) 2.2067(12) Å]. These values are comparable with the corresponding values [2.280(2), 2.261(2), 2.198(2) Å] in [$RuCl_2$(TTP)] [22] and [2.306(1), 2.276(2), 2.212(2) Å] in [$RuCl_2$(CyTTP)]·$2Me_2SO$ [23]. These distances are also close to the respective values observed in [$RuCl_2$(ETP)($MeCN)_3$]·$2CF_3SO_3$ [2.314(6), 2.309(6), 2.261(6) Å] [22], [$RuCl_2$(ETP)$_2$]·$CHCl_3$·Et_2 [2.389, 2.358, 2.295 Å] [24], [$RuCl_2$(ETP)(Me_2 SO)]·$C_6H_5Me_5$ [2.366, 2.289, 2.257 Å] [25], [$RuCl_2$(CMTP)(PPh_3)] [2.350(1), 2.320(1), 2.308(1) Å] [27], [R_2Cl_3(ETP)]BPh_4·$CHCl_3$·$0.5H_2O$ [2.308, 2.292, 2.252 Å] [28] and [Ru_2Cl_3(ETP)]·CF_3SO_3·CH_2Cl_2 [2.287(2), 2.266(2), 2.251(2) Å] [22]. Examination of the Ru–P distances in all the above compounds suggests that the distances involving the two terminal (basal) atoms are always longer than that involving the central atom. Although the small differences in the two basal bonds could be attributed to steric factors, the shortening of the apical bonds are most probably due to electronic effects and certainly consistent with the suggestion that there should be strong π-bonding in square pyramidal type metal complexes [35]. It should be noted, however, that in the $[Ru_2Cl_3(TRIPHOS)_2]^+$ cation, which contains sterically rigid tripodal PPP ligands, all the Ru–P distances are virtually identical [2.296(3)–2.310(3), average 2.305 Å] [29].

The Ru–Cl two distances in the present complex [2.3838(13), 2.3903(11) Å] are nearly the same, but those in the related complexes $RuCl_2$(TTP)][2.394(2), 2.439(2) Å] [22] and [$RuCl_2$(CyTTP)]·$2Me_2SO$ [2.406(2), 2.455(1) Å] [23] are distinctly different, the longer bond in each case being *trans* to a phosphorus

donor atom. The average value in the present complex [2.3871 Å] is shorter the average values in these two complexes, 2.416 and 2.430 Å, respectively, but comparable with those in the monomeric five-coordinate complexes $[RuCl_2(PPh_3)_3]$[2.387 Å] [36] and $[RuCl_2\{PPh_2(CH_2SiMe_3)\}_3]$ [2.392 Å] [37].

The geometry parameters involving the triphosfer ligand are basically as expected. However, the relative orientations of the two ferrocenyl moieties with respect to the RuP_2 chelate planes are significantly different, as indicated by the different values for the equivalent torsion angles, Ru(1)–P(1)–C(1)–Fe(1) 25.0(4) and Ru(1)–P(3)–C(16)–Fe(2) −51.7(3)°, and Ru(1)–P(2)–C(11)–Fe(1) −26.5(4)° and Ru(1)–P(2)–C(11)–Fe(2) −7.1(3)°. The Fe–C(Cp) distances vary from 2.019(5) to 2.055(5), average 2.040 Å, and are comparable with those in the related ferrocenyl–bis(phosphine) palladium complex $[PdBr(C_{14}H_8Cl)\{Fe(C_5H_4–PPh_2)_2\}]$ [1.976(9)–2.048(8), average 2.014 Å] [21] and ferrocenyl–anthracene complex $[Fe(C_5H_4–C_{14}H_9)_2]$ [2.023(4)–2.083(4), average 2.047 Å] [21]. The two Cp rings around both iron atoms in the present complex are almost parallel as indicated by the dihedral angles 4.1(4) [for Fe(1)] and 2.7(3)° [for Fe(2)]. However, the Cp rings around Fe(1) are almost eclipsed, whilst those around Fe(2) are ca. 35° rotated from a totally eclipsed arrangement. The bond lengths and angles in all the Cp rings are as expected with minor deviations from ideal pentagon due to the strain suffered by bonding with the phosphorus atoms. In particular the bonds involving the phosphorus bonded carbon atoms are slightly but definitely lengthened compared with the other C–C bonds as indicated by their average values 1.434 versus 1.413 Å. The C–C–C angles at these atoms are also slightly smaller than those at other carbon atoms [106.2(4)–107.0(4), average 106.7° vs. 107.5(4)–109.2(4), average 108.3°]. Similar distortions of the Cp rings due to anthracenyl substituents were also observed in the above mentioned $[Fe(C_5H_4–C_{14}H_9)_2]$ complex [21]. The phenyl rings also suffer some distortions from ideal hexagon, mainly at the carbon bonded to phosphorus; the C–C–C internal angles for these atoms are all slightly narrower [117.4(4)–119.6(5), average 118.2°] than the ideal value 120°.

It has been mentioned earlier that the ruthenium metal in the present compound has a five-coordinate square pyramidal coordination; however, it is also of interest to note that one of the phenyl hydrogens [H(32)] makes a close approach to the metal, from the opposite side of P(2), within 2.89 and this gives it a pseudo-octahedral environment. This Ru(1)···H(32) contact is significant in that it blocks the unused octahedral site of the metal centre. Similar situation, also observed in other cases, e.g. $[RuCl_2(PPh_3)_3]$ [36] and $[RhBr(1\text{-naphthyl})_2(PPh_3)_2]$ [38], has been suggested to give extra stability to the electron deficient metal centres in such species [38].

Acknowledgements

The NMR spectra were recorded by Eric Lewis of the University of Wales, Bangor whom I.R. Butler gratefully thanks. Elemental analyses were performed in the same department by G. Connolly. He also thanks the EU for funding the Erasmus placement of U. Griesbach. The high resolution mass spectra were obtained at the EPSRC central research facility at the University of Wales, Swansea and he gratefully thanks the staff who performed the analyses. P. Zanello gratefully acknowledges the financial support of the University of Siena (ex quota 60%). Thanks are due to G. Montomoli for her technical assistance. Finally I.R. Butler acknowledges the patience of his research group allowing him to carry out much of this synthetic work, particularly S. Quayle, G. Kelly and J. Szewczyk. A loan of $RuCl_3 \cdot xH_2O$ from Johnson-Mathey p.l.c. is gratefully acknowledged.

References

[1] G.P. Sollot, J.L. Snead, S. Portnoy, W.R. Peterson Jr., H.E. Mertwoy, Chem. Abstr. 63 (1965) 18147b.
[2] J.J. Bishop, A. Davison, M.L. Katcher, D.W. Lichtenberg, R.E. Merrill, J.C. Smart, J. Organomet. Chem. 27 (1971) 241.
[3] A. Togni, T. Hayashi, editors. Ferrocenes. Weinheim: VCH Press, 1995.
[4] (a) W.R. Cullen, J.D. Woolins, Coord. Chem. Rev. 39 (1981) 1. (b) W.R. Cullen, S.J. Rettig, T.-C. Zheng, Organometallics 11 (1992) 277. (c) A. Togni, G. Rihs, R.E. Blumer, Organometallics 11 (1992) 613. (d) T.S.A. Hor, L.-T. Phang, Polyhedron 9 (1990) 2305. (e) T.S.A. Hor, S.P. Neo, C.S. Tan, T.C.W. Mak, K.W.P. Leung, R.-J. Wang, Inorg. Chem. 31 (1992) 4510. (f) M.I. Bruce, P.A. Humphrey, O. Shawkataly, M.R. Snow, E.R.T. Tiekint, W.R. Cullen, Organometallics 9 (1990) 2910. (g) S.T. Chacon, W.R. Cullen, M.I. Bruce, O. Shawkataly, F.W.B. Einstein, R.H. Jones, A.C. Wilkes, Can. J. Chem. 68 (1990) 2001. (h) M. Sato, M. Sekino, J. Organomet. Chem. 444 (1993) 185. (i) T. Hayashi, A. Yamamoto, Y. Ito, E. Nishioka, H. Miura, K. Yanagi, J. Am. Chem. Soc. 14 (1989) 6301. (j) I.R. Butler, W.R. Cullen, T.-J. Kim, S.J. Rettig, J. Trotter, Organometallics 4 (1985) 972.
[5] C.R.S.M. Hampton, I.R. Butler, W.R. Cullen, B.R. James, J.P. Charland, J. Simpson, Inorg. Chem. 31 (1992) 5509.
[6] (a) I.R. Butler, R.L. Davies, Synthesis (1996) 1350. (b) I.R. Butler, S. Sellarajah, Undergraduate Dissertation, University of Wales, 1996.
[7] A. Togni, M. Hobi, G. Rihs, G. Rist, A. Albinati, D. Zech, H. Keller, Organometallics 13 (1994) 1224.
[8] R. Holm, Inorg. Synth. 12 (1971) 238.
[9] J.A. Darr, S.R. Drake, M.B. Hursthouse, K.M.A. Malik, Inorg. Chem. 32 (1993) 5704.
[10] N.P.C. Walker, D. Stuart. DIFABS Program for Absorption Correction, Acta Crystallogr. Sect. A 39 (1983) 158; adapted for FAST geometry by A.I. Karaulov, University of Wales Cardiff, 1991.
[11] G.M. Sheldrick, SHELXS86 program for crystal structure solution, Acta Crystallogr. Sect. A 46 (1990) 467.
[12] G.M. Sheldrick, SHELXL93 program for crystal structure refinement, University of Göttingen, Germany, 1993.
[13] K. Davies, SNOOPI program for crystal structure drawing, University of Oxford, UK, 1983.
[14] M.M. Taquikhan, R. Mohiuddina J. Coord. Chem. 6 (1977) 171 and references therein.

[15] (a) X.-L. Luo, R.H. Crabtree, J. Chem. Soc. Dalton Trans. (1991) 587. (b) M.T. Costello, P.E. Fanwick, M.A. Green, R.A. Walton, Inorg. Chem. 31 (1992) 2359. (c) S.A. Westcott, G. Stringer, S. Anderson, N.J. Taylor, T.B. Marder, Inorg. Chem. 33 (1994) 4589.
[16] (a) D. Michos, X.-L. Luo, R.H. Crabtree, Inorg. Chem. 31 (1992) 4245. (b) C. Bianchini, P.J. Perez, M. Peruzzini, F. Zanobini, A. Vacca, Inorg. Chem. 30 (1991) 279.
[17] J.C. Kotz, C.L. Nivert, J.M. Lieber, R.C. Reed, J. Organomet. Chem. 91 (1975) 87.
[18] A. Houlton, P.T. Bishop, R.M.G. Roberts, J. Silver, J. Organomet. Chem. 364 (1989) 381.
[19] P. Zanello, G. Opromolla, G. Giorgi, G. Sasso, A. Togni, J. Organomet. Chem. 506 (1996) 61 and references therein.
[20] (a) M.D. Ward, Chem. Soc. Rev. (1995) 121. (b) R.R. Gagné, C.A. Kowal, T.J. Smith, M.C. Cimolind, J. Am. Chem. Soc. 101 (1979) 4571. (c) A.W. Bott, Current Separations, Bioanalyt. Syst. 16 (1997) 61.
[21] I.R. Butler, L.J. Hobson, S.J. Coles, M.B. Hursthouse, K.M.A. Malik, J. Organomet. Chem. 540 (1997) 27.
[22] A. Albianati, Qiongzhong Jiang, H. Ruegger, L.M. Venanzi, Inorg. Chem. 32 (1993) 4940.
[23] G. Jia, I. Lee, D.W. Meek, J.C. Gallucci, Inorg. Chim. Acta 177 (1990) 81.
[24] R.R. Guimerans, E.C. Hernandez, M.M. Olmstead, A.L. Balch, Inorg. Chim. Acta 165 (1989) 45.
[25] G. Delgado, A.V. Rivera, T. Suarez, B. Fontal, Inorg. Chim. Acta 233 (1995) 145.
[26] I. Dahlenburg, S. Kerstan, D. Werner, J. Organomet. Chem. 411 (1991) 457.
[27] L. Solujic, E.B. Milosavijevic, J.H. Nelson, N.W. Alcock, J. Fischer, Inorg. Chem. 28 (1989) 3453.
[28] W.S. Sheldrick, K. Brandt, Inorg. Chim. Acta 217 (1994) 51.
[29] R.F. Rhodes, C. Sorato, L.M. Venanzi, F. Bachechi, Inorg. Chem. 26 (1987) 604.
[30] D.W. Krassowski, J.H. Nelson, K.R. Brower, D. Hauenstein, R.A. Jacobson, Inorg. Chem. 27 (1988) 4294.
[31] J. Halpern, C.S. Wong, J. Chem. Soc. Chem. Comm. (1973) 629.
[32] B.R. James, L.O. Markham, Inorg. Chem. 13 (1974) 97.
[33] P.S. Halmann, B.R. McGarvey, G. Wilkinson, J. Chem. Soc. A (1968) 3143.
[34] T.A. Stephenson, G. Wilkinson, Inorg. Nucl. Chem. 28 (1966) 945.
[35] M.R.M. Fontes, G. Oliva, L.A.C. Cordeiro, A.A. Batista, J. Coord. Chem. 30 (1993) 125.
[36] S.J.L. Placa, J.A. Ibers, Inorg. Chem. 4 (1965) 778.
[37] F.A. Cotton, M. Matusz, Inorg. Chim. Acta 131 (1987) 213.
[38] J. Chatt, A.E, Underhill, J. Chem. Soc. (1963) 2088.